Astron. Astrophys. 324, 651–655 (1997)

ASTRONOMY
AND
ASTROPHYSICS

Case studies for planetary nebulae with tilted axes

W. Saurer⋆

Institut für Astronomie, Leopold-Franzens-Universität, Innsbruck Technikerstr. 25, A-6020 Innsbruck, Austria

Received 23 October 1996 / Accepted 2 December 1996

Abstract. In this paper we discuss the morphology of two elliptical, point-symmetric planetary nebulae (PNe) with tilted axes: M1-79 and Wei 1-5. By means of simple geometry and the assumption of optical thinness in [OIII] we were able to reproduce the observational (morphological) data on these two objects. We have constructed three-dimensional models consisting of an inner and an outer ellipsoid which can account for the overall shape, the tilt of the axes, and the intensity distribution of the PNe when looked at a certain viewing angle. Our results can be interpreted as an indication for a non-circular component of the density distribution within the equatorial plane.

Key words: planetary nebulae: general – planetary nebulae: individual: M1-79, Wei 1-5

1. Introduction

After a certain time of recession, investigating the morphologies of planetary nebulae (PNe) has been regenerated again to a most up-to-date and attractive topic in recent years. The rapid development of improved detectors and computing facilities and the extensive morphological inventory has put astronomers in the position of a forced understanding of the variety of shapes in which PNe appear. Based on a great number of articles which can be regarded as pioneering work (e.g. Curtis 1918; Perek & Kohoutek 1967; Acker et al. 1992; Kwok et al. 1978; Balick 1987, to name only a few) morphological classification schemes and hydrodynamical methods of calculation have been developed and proposed which put successfully together theoretical knowledge/expectations with observational data (e.g. Mellema et al. 1991; Icke et al. 1992; Frank et al. 1993, Stanghellini et al. 1993; Corradi & Schwarz 1995, Pascoli 1995). For a short summary of this history see Manchado et al. (1996a). The most widely classification common to all schemes is based on the projected shape of the object: round, elliptical, and bipolar. Two additional criteria were brought into discussion very recently. Schwarz et al. (1993) introduced the concept of point-symmetry, and Manchado et al. (1996b) defined the new class of quadrupolar PNe.

In this work we will treat two members of a special species of elliptical PNe. The characteristics of elliptical PNe can be described by (usually) well defined geometrical major and minor axes (which are, by definition, perpendicular to each other). A third axis can be defined which connects the two intensity enhancements that are common to almost all elliptical PNe. As a matter of fact this third axis (intensity axis) coincides with the minor axes for the majority of elliptical PNe (and, in a few cases, with the major axis). However, there is a small but noticeable number of PNe for which the intensity axis and the geometrical minor axis are tilted considerably.

The aim of this paper is to investigate if and how simple geometrical projection effects can account for these tilts.

2. Observations

The direct images were obtained with the 2.2 m telescope on Calar Alto in October 1989 with a RCA (SID 006 EX) detector (pixelsize 15 μm^2, which corresponds to a spatial resolution of $0\farcs17^2$ per pixel). The interference filters used for these observations ([OIII], Hα+ [NII]) were centered at 5005 Å and 6574 Å with pass bands of 90 Å and 104 Å, respectively. The exposure time for both images was 1 800 sec. After applying standard reduction procedures (bias, flatfielding) the images were corrected for bad columns using an intensity dependent mask which was derived from flatfields.

3. The model

The standard spatio(-kinematical) model for elliptical PNe can be understood as an inevitable consequence of the adopted process of forming (interacting winds model, Kwok et al. 1978) – and vice versa. These PNe are commonly believed to be the product of non-isotropical wind ejecta from the progenitor star. For details of the formation and evolution see Balick et al. (1987). Theory and observations seem to agree very well for this kind of objects. The scenario starts with a low– to intermediate mass star during the Asymptotic Giant Branch phase. A fast

Send offprint requests to: Walter.Saurer@uibk.ac.at

⋆ Visiting Astronomer at the Centro Astronomico Hispano-Aleman, Calar Alto, operated by the Max-Planck-Institut für Astronomie, Heidelberg, jointly with the Spanish National Commission for Astronomy.

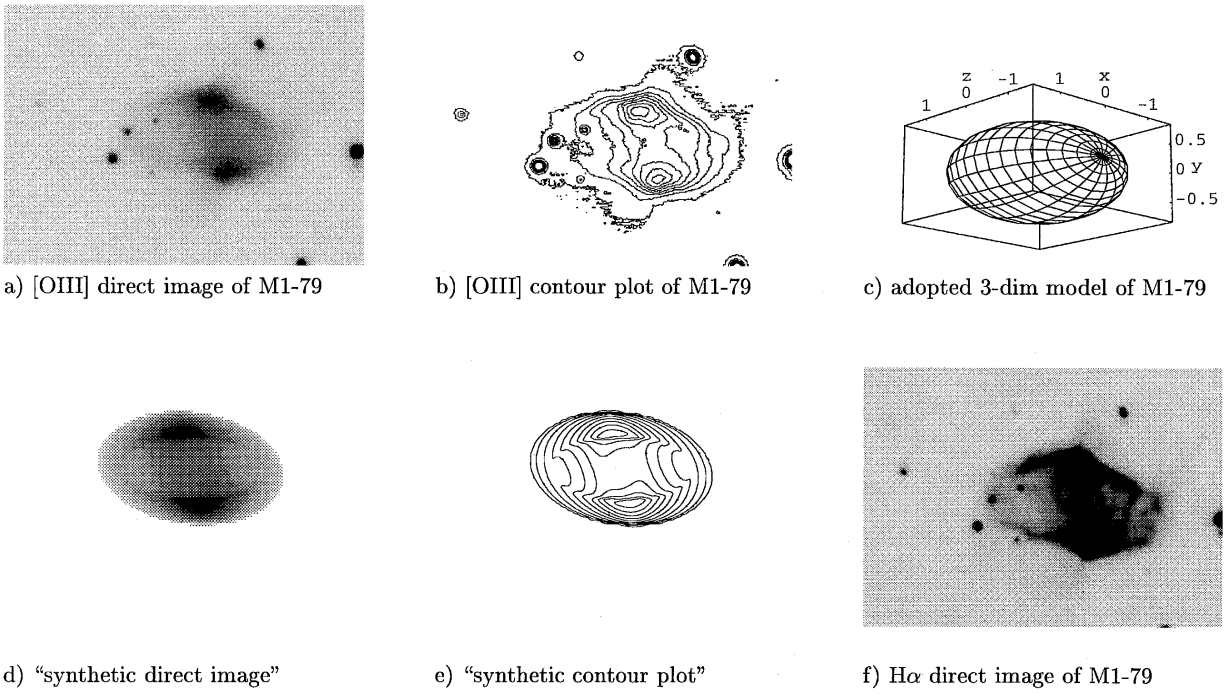

a) [OIII] direct image of M1-79 b) [OIII] contour plot of M1-79 c) adopted 3-dim model of M1-79

d) "synthetic direct image" e) "synthetic contour plot" f) Hα direct image of M1-79

Fig. 1. Model versus observation for M1-79. The direct images have a size of $80'' \times 60''$, North is to the top and East to the left

wind drives a shock wave into a former slow wind. The visible shell of the PN is the photoionised region between the outward-facing shock and a contact discontinuity following this shock (Mellema et al. 1991). If the slow wind exhibits an equatorial density excess the outer shock can be shaped prolate-spheroidal (Kahn & West 1985; Icke 1988). The projection onto the sky will give an ellipse with density (intensity) enhancements at the two ends of the minor axis due to the torus-like structure in the equatorial plane of the three-dimensional ellipsoid. The equatorial density excess can be caused by a multiple star system but, as was shown very recently, even by a single rotating star (Dorfi & Höfner 1996).

Following this general concept we describe the shell of an elliptical PN in our modelling by two ellipsoids with the same center and having the same directions of the main axes. One ellipsoid is positioned completely inside the other one. The shell is now defined as the volume inside the outer ellipsoid and outside the inner ellipsoid. This idea was first introduced by Bässgen et al. (1990) who used two ellipsoids with two axes each and their ionisation model successfully to reproduce the projected appearance of NGC 3132.

We designate the ellipsoids with $E_i(a_i, b_i, c_i)$ where a, b, c are the semi-diameters in x, y, z direction, respectively, and i = 1 (inner ellipsoid) or 2 (outer ellipsoid). The density (ρ) within the shell is assumed to decrease exponentially along the |z|-axis to simulate the equatorial density excess (hence the equatorial plane is fixed within the x–y plane). We then calculated the projected intensity distribution of this volume onto the sky for different viewing angles to generate "synthetic observations" of our model. The calculations were done by integrating the density within the adopted PN-volume along the line of sight. This procedure will give a rough approximation of what is observed implying an optically thin PN without internal extinction (and constant temperature). To compare the model with real observations we have chosen the [OIII] line which can be assumed to satisfy the condition of optical thinness. The line of sight is defined with two angles: α is the angle within the x–y plane ($\alpha = 0^\circ$ means looking along the x-axis), and β is defined as the angle between the x–y plane and the line of sight.

To find the best fit to the observations we have referred to three characteristics of the projection of the model: the overall shape, i.e. the parameters of the projected ellipse, the tilt between the minor and the intensity axis, and the intensity distribution within the projection represented by the distribution along a cut through the two intensity enhancements. The model-parameters to change are a_i, b_i, c_i, the viewing angle (α, β), and the exponential decrease of the density along the |z|-axis.

4. Results, individual objects

First we note an obvious, but nevertheless important result. Models with symmetry on rotation about the z-axis (i.e. $a_1 = b_1$, $a_2 = b_2$) will not (for no viewing angle) yield a tilt between the minor and the intensity-axis of the projected ellipses. At least one ellipsoid has to be three-axial (or at least $a \neq b$ with the designations used here). This feature can be seen also in articles that have presented more elaborate models and their projections to the sky with different viewing angles (e.g. Pascoli 1990; Frank 1993). Two-dimensional calculations therefore cannot explain these tilted angles up to now – assuming that they are caused by

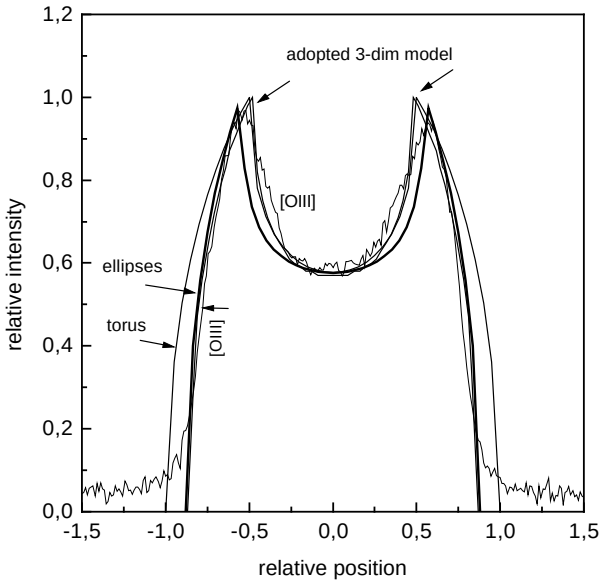

Fig. 2. A cut through the two intensity enhancements of M1-79

projection effects. To our knowledge, fully three-dimensional calculations were carried out successfully only very recently (Cliffe et al. 1995). However, when we calculate projections with the above mentioned symmetry, we can reproduce a great variety of observational shapes of elliptical PNe with our model.

4.1. M1-79 (PN G093.3–02.4)

Fig. 1 a, b gives a direct image and a contour plot of the PN M1-79 in the line [OIII]. We have decided to give both these illustrations because the contour plots give more information on the density distribution within the objects but they are less appropriate to show the visible appearance of the nebulae. This PN appears as a point-symmetric elliptical PN. The projected major axis of this object has a position angle (P.A.) of $\approx 85°$and the intensity enhancements exhibit a P.A. of $\approx 14°$, hence they are tilted to the minor axis with 19°. The ratio of the projected major and minor axis is ≈ 1.6 measured at the outermost elliptical contour in Fig. 1 b. In finding a model for this PN we start with a cut through the intensity enhancements. The result is shown in Fig. 2.

Fig. 2 shows the wellknown double-peaked structure which can be interpreted in terms of a torus-like shell seen almost edge-on. The fit labeled "torus" was achieved with the assumption of a torus seen edge on, disregarding the three-dimensional shape of the object. A best fit requires an inner radius of 0.5 and an outer radius of 1. Although the torus can explain the intensity distribution within the inner part rather well, the wings of the fit seem to be too convex. One possibility to steepen the gradient in this region is the assumption of a distorted torus which can be realised by substituting the two rings with two ellipses. We have to mention here that the steepening can also be caused by interaction with the interstellar medium. Because we want to generate only a geometrical model and, in addition, we cannot decide on this problem here, we accept the two ellipses as a working hypothesis. The fit is shown in Fig. 2, too, designated with "ellipses". The two ellipses giving this fit are seen "edge on" and both are elongated along the line of sight (major axes 1, 0.55; minor axes 0.8, 0.5 for the outer and inner ellipse, respectively). For reasons of comparison and without loss of generality all curves are scaled along the abszissa in Fig. 2 by a constant factor to let the two peaks coincide and along the ordinate to let the peaks approximately be 1 (the scaling was done only approximately to make the curves more distinguishable in the diagram).

Using these values as a first approximation we can proceed to find a three-dimensional model for M1-79. Our result in finding a best fit both to Fig. 1 a, b, and Fig. 2 is E_1(0.6, 0.5, 1.2), E_2(1.5, 0.8, 1.5), α=20°, and β=20°, and $\rho \propto e^{-|z|}$. Values of α=–20°, β=–20°will give the same result and we cannot decide on this here (roughly speaking, this corresponds to seeing the ellipsoid from above or below where the direction is given with the z-axis). Giving the two angles opposite signs this will result in a mirrored image of the projection. The projection of this model is shown in Fig. 1 d, e. As can be seen, the visual appearance and other characteristics of this PN can be reproduced with the model. The point-symmetry, the overall shape and the equatorial waist can be found in the projection. The ratio of the major to minor axis of the projected model is ≈ 1.6, the P.A. of the projected ellipse is $\approx 15°$and the P.A. of the intensity enhancements is $\approx 83°$. Hence these numbers are in good agreement with the observations. The cut through the two intensity enhancements of the projected model is also drawn into Fig. 2 and fits strikingly well. Along the wings it is following the ellipses fit and in the inner part it almost coincides with the torus fit. In addition, the shapes of the contours can be reproduced. In Fig. 1 c we present the outer ellipsoid of our adopted three-dimensional model of M1-79. In this representation the plane of the sheet is identical to the plane perpendicular to the line of sight, so the observer is looking at the ellipsoid as it is.

In Fig. 1 f we present a direct image of M1-79 obtained in the light of Hα + [NII]. The global appearance remains the same as in [OIII]. However, two additional lobes can be seen more clearly than in Fig. 1 a. These lobes, extending to the northwest and southeast direction with a P.A. of ≈–40°appear point-symmetric, too. They are defining an additional symmetry axis for this PN. We have used this image for an additional verification of our modelling. The cut through the intensity enhancements in Hα+[NII] was achieved by integrating the square of the density along the line of sight within the shell. The result of these calculations coincides with the measured brightness distribution within the inner part of the PN with an accuracy identical to that of Fig. 2. Especially the intensity ratio between the peak and the central trough, which is higher in Hα+[NII] than in [OIII], is reproduced. However, in the outer parts the intensity is increasing more rapidly than the model would predict. Fig. 1 f reveals unusual sharp edges of this PN in the light of Hα+[NII] and at the two longer edges the lobes seem to come out. In this region maybe the geometrical effects are superimposed with others.

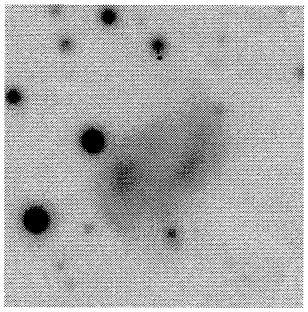

a) direct image of Wei 1-5

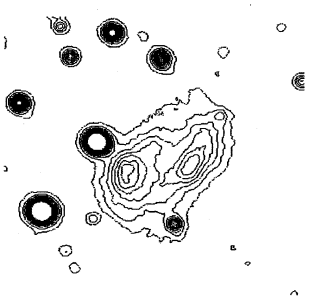

b) contour plot of Wei 1-5

c) "synthetic direct image"

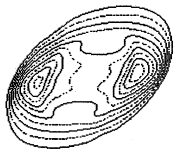

d) "synthetic contour plot"

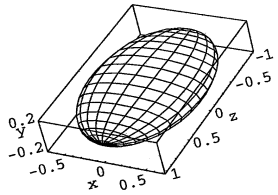

e) adopted 3-dim model

Fig. 3. Model versus observation for Wei 1-5. The direct image has a size of $107'' \times 107''$, North is to the top and East to the left

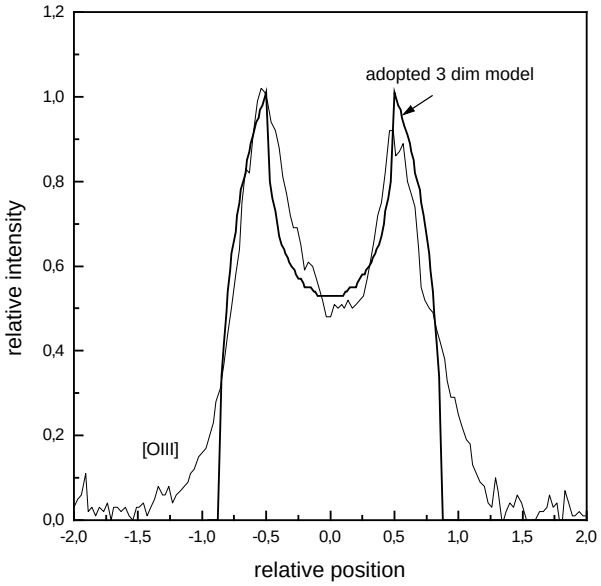

Fig. 4. A cut through the two intensity enhancements of Wei 1-5

4.2. Wei 1-5 (PN G013.7–15.3)

This object is a very recent addition to the family of PNe. It was detected by Weinberger (1995) and proved as a PN by Kerber & Claeskens (1996) who have already published the contour plot of Wei 1-5. For the reason of completeness we will again show it here. Also this PN exhibits point-symmetry. In Fig. 3 we present the direct imaging in [OIII], the contour plots and the modelling for Wei 1-5 as described for M1-79. The observation was kindly placed at our disposal by Kerber & Claeskens who have already achieved a torus fit for this object.

Our result for the three-dimensional shape of this PN is E_1(0.4, 0.1, 0.5), E_2(0.7, 0.2, 1.0), for the viewing angle α=50°and β=40°, and $\rho \propto e^{-2\cdot|z|}$. The tilt between the minor axis and the intensity axis is ≈45°both for the observation and the projected model. The ratio of the projected major and minor axis is 1.7 for the model and the observation (measured at the outermost contour line). The fit of the intensity distribution is shown in Fig. 4. Again, this fit can be regarded as satisfactory. For Wei 1-5, our model can also account for the measured intensity distribution along the intensity axis in Hα+[NII] (which was published in Kerber & Claeskens (1996)). With the assumption of similar density distribution of hydrogen and oxygen this can be interpreted as optical thinness of the shell also in the light of Hα+[NII].

5. Discussion and conclusion

We were able to reproduce direct images for two elliptical and point-symmetric PNe with tilted axes by using three-dimensional models. For this aim we have applied only geometrical projection effects. At a first glance our results seem to be rather peculiar and not compatible with the (two-dimensional) scenario of the formation of elliptical PNe. If our assumption of optical thinness in [OIII] holds, a necessary condition for introducing tilted angles is a non-axial model with respect to the polar axis. Our result is an elliptical shape of the PNe even in the equatorial plane. This implies an additional preferential direction (for the density distribution and/or for the geometrical shape of the slow wind) which is situated within the equatorial plane (in addition to the polar direction). The reasons for this can, at present time, only be suspected speculatively. The scenarios of double and triple star systems are discussed briefly in Manchado et al. (1996b), but the consequences of, e.g. precession, ellipticity of orbits, tidal effects on the equatorial disk and hence on the formation process of PNe are not studied in detail up to now, at least not three-dimensional. Further possible reasons can be found in the interaction with the surrounding interstellar medium or with formerly ejected material from the AGB star. At least for one PN (M1-79) the two additional lobes in Fig. 1 f give us some indication that it was produced by a binary star.

Besides other features concerning the morphology of PNe, also tilted axes, as introduced here, can be regarded as strongly dependent on the filters used for direct imaging and on the exposure times applied for the observations. In this way they can change with subsequent investigations and so the results will change. Our assumptions are very restricting (optical thinness, no extinction, constant temperature and, as a very important fact, the assumption that the two density enhancements originate from a closed ringlike feature) and the method used is only based on fundamental geometry. However, it seems that tilted axes can give an indication for a non-circular density distribution within the equatorial plane during the evolution of elliptical PNe assuming these simplifications.

The feature of tilted axes is not only restricted to the two PNe we have treated here. We have searched the catalogues of Manchado et al. (1996a) and Schwarz et al. (1992) for similar objects. MaC1-13, M3-34, K3-38, K3-34, We 1-9, M1-75, We 1-11, M2-52, M2-53, A 2, Ba 1, and Hb4, A47 turned out to be good candidates for belonging to this group, mostly due to their appearance in the light of [OIII].

Acknowledgements. The author is grateful to Prof. R. Weinberger for helpful discussions and carefully reading the manuscript and to F. Kerber and J.-F. Claeskens who have kindly placed the [OIII] direct image of Wei 1-5 to our disposal. We also would like to thank for observing time at the 2.2 m telescope of the German-Spanish Calar Alto Observatory. For their helpfulness special thanks go to the staff of this observatory. This work was supported financially by the "Österreichische Forschungsgemeinschaft, project number 06/1006 (travelling costs) and by the "Jubiläumsfonds der Österreichischen Nationalbank", project number 4713 (computer facilities).

References

Acker A., Ochsenbein F., Stenholm B., Tylenda R., Marcout J., Schohn C., 1992, Strasbourg-ESO Catalogue of Galactic Planetary Nebulae, Garching, ESO
Balick B., 1987, AJ 94, 671
Balick B., Preston H.L., Icke V., 1987, AJ 94, 1641
Bässgen M., Diesch C., Grewing M., 1990, A&A 237, 201
Cliffe J.A., Frank A., Livio M., Jones T.W., 1995, ApJ 447, L49
Corradi R.L.M., Schwarz H.E., 1995, A&A 293, 871
Curtis H.D., 1918, Publ. Lick Obs., 13, 55
Dorfi, E.A., Höfner S., 1996,A&A 313, 605
Frank A., Balick B., Icke V., Mellema G., 1993, ApJ 404, L25
Icke V., 1988, A&A 202, 177
Icke V., Balick B., Frank A., 1992, A&A 253, 224
Kahn F.D., West K.A., 1985, MNRAS 212, 837
Kerber F., Claeskens J.-F., 1996, A&A in press
Kwok S., Purton C.R., Fitzgerald M.P., 1978, ApJ 219, L125
Manchado A., Guerrero M.A., Stanghellini L., Serra-Ricart M., 1996a, The IAC Morphological Catalog of Northern Galactic Planetary Nebulae, Instituto de Astrofísica de Canarias
Manchado A., Stanghellini L., Guerrero M.A., 1996b, ApJ 466, L95
Mellema G., Eulderink F., Icke V., 1991, A&A 252, 718
Pascoli G., 1990, A&A 232, 184
Pascoli G., 1995, Ap&SS 234, 281
Perek, L.,Kohoutek L., 1967, Catalogue of Galactic Planetary Nebulae, Prague, Czechoslovakian Academy of Science
Schwarz H.E., Corradi R.L.M., Melnick J., 1992, A&AS 96, 23
Schwarz H.E., Corradi R.L.M., Stanghellini L., 1993, in IAU Symp. 155: Planetary Nebulae, R. Weinberger, A. Acker eds., Kluwer, Dordrecht, p. 214
Stanghellini L., Corradi R.L.M., Schwarz H.E., 1993, A&A 276, 463
Weinberger, R., 1995, PASP 107, 58

This article was processed by the author using Springer-Verlag LaTeX A&A style file *L-AA* version 3.